AD NUMBER

AD461486

NEW LIMITATION CHANGE

TO

Approved for public release, distribution unlimited

FROM

Distribution: Further dissemination only as directed by Army Electronics Research and Development Lab, Fort Monmouth, NJ 07703; Jan 1965 or higher DoD authority.

AUTHORITY

AEC ltr dtd 24 Jan 1966

STUDY OF EFFECT OF HIGH-INTENSITY PULSED NUCLEAR RADIATION ON ELECTRONIC PARTS AND MATERIALS (SCORRE)

REPORT NO. 1
SIGNAL CORPS
CONTRACT NO. DA28-043-AMC-00212(E)
DEPARTMENT OF THE ARMY
FIRST SEMIANNUAL PROGRESS REPORT
15 JUNE 1964 - 31 DECEMBER 1964

U. S. ARMY SIGNAL RESEARCH AND
DEVELOPMENT LABORATORY
FORT MONMOUTH, NEW JERSEY

IBM FSD Space Guidance Center Owego, New York

This page for INTERNAL DISTRIBUTION only.
Please remove prior to external distribution.

Semiannual Progress Report

STUDY OF EFFECT OF

HIGH-INTENSITY

PULSED NUCLEAR

RADIATION

ON

ELECTRONIC PARTS

AND MATERIALS

(SCORRE)

IBM NO.: 65-521-05

DATE: 19 January 1965

ORIGINATOR: Radiation Effects Staff

CONTENT APPROVED BY:

W. A. Bohan

CONTRACT NO.:

DA28-043-AMC-00212(E)

Internal Distribution

W. A. Bohan
J. T. Caulfield
F. A. Frankovsky
M. Shatzkes

IBM

FSD SPACE GUIDANCE CENTER
OWEGO NEW YORK

STUDY OF EFFECT OF HIGH-INTENSITY PULSED NUCLEAR RADIATION ON ELECTRONIC PARTS AND MATERIALS (SCORRE)

First Semiannual Progress Report
15 June 1964 to 31 December 1964
Contract No. DA28-043-AMC-00212(E)

ORIGINATOR: Radiation Effects Staff

APPROVED BY: [signature]

IBM NO. : 65-521-05

Objective:

To study the effects of high-intensity pulsed nuclear radiation exposure on selected parts and materials used in critical high-speed electronic circuitry.

"This research on transient radiation effects on electronics is sponsored by the Defense Atomic Support Agency and is conducted under the technical guidance of the United States Army Electronics Research and Development Laboratory, Fort Monmouth, New Jersey, 07703, and the DASA-TREE Project Officer."

International Business Machines Corporation
Federal Systems Division
Owego, New York

TABLE OF CONTENTS

Table of Contents (cont)

LIST OF ILLUSTRATIONS

PURPOSE

The purpose of work described in this report is to determine the effects of high intensity nuclear radiation on the following electronic components and materials:

- Capacitors
- Thin Film Resistors
- Magnetic Tapes
- Magnetic Cores.

ABSTRACT

Radiation testing of ceramic, glass, tantalum, mica, polystyrene, and mylar capacitors is complete. Data analysis is not complete. New effects were observed when testing glass and tantalum capacitors.

Leakage currents in irradiated thin film resistors are principally due to secondary emission and air ionization.

No data errors were detected on a magnetic tape that was irradiated.

Dosimetry techniques are described, and errors in previous linac dosimetry are discussed.

Section I

INTRODUCTION

Section I

INTRODUCTION

This is the Contract No. DA 28-043-AMC-00212(E) semiannual report for the June to December 1964 period. During this period, tests were conducted at the Sandia Pulsed Reactor Facility (SPRF) and on the linear accelerator (linac) at General Atomics, San Diego, California. In these tests, various aspects of radiation effects were measured in mylar, polystyrene, tantalum oxide, mica, ceramic, and glass capacitors. Also, the effects of high intensity pulsed radiation on magnetic cores and tapes were measured, and an experiment was performed to determine the pulsed radiation effects on thin film resistors.

During the reporting period, IBM's major effort was planning and performing the SPRF and linac tests. Data accumulated in these tests include over 800 oscilloscope photographs of capacitor responses — about 200 at SPRF and 600 at the General Atomics' linac. Irradiation of one magnetic tape and two memory core planes and the required dosimetric measurements at the General Atomics' linac are represented by about 250 oscilloscope photographs and 1,250 determinations. Reduction of the raw data is complete for the SPRF tests and is in progress for the linac tests. Thus, except for the experiment on thin-film resistors conducted during the earlier linac tests, the conclusions in this report must be considered preliminary.

Test data are presented in Section II. This section is subdivided into four subsections: SPRF Test, Linac Test, Thin Film Studies, and Magnetic Tapes and Core Irradiation. Descriptions of the linac dosimetry and the dosimetry used in the shielded capacitor experiments at the SPRF are given in Section III. Instrumentation techniques and routine dosimetric procedures are not included because this information was discussed in Reference 1 and other previous reports.

Section II

TEST DATA

Section II

TEST DATA

A. SPRF TEST

Mylar and polystyrene capacitors were tested at the SPRF to determine the dependence of radiation effects on capacitor geometry, applied voltage, dose rate, and repeated irradiation. Also included in this test were experiments to learn the relative effectiveness of neutron and gamma radiation in inducing currents in mylar, polystyrene, glass, solid tantalum, ceramic, and mica capacitors.

The mylar and polystyrene capacitors tested cover the entire range of capacitance values and voltage ratings available for each type. These capacitors are listed in Tables 1 and 2.

The testing was conducted to gather data on the radiation-induced current from three separate effects:

- Variation of voltage, capacitance, and d-c working voltage (WVDC)
- Repeated irradiation
- Alteration of the neutron-gamma ray ratio

Tables 3 and 4 list the number of capacitor types tested for each effect and the number that yielded usable oscillographs for analysis.

1. NORMAL VARIATIONS OF VOLTAGE, CAPACITANCE, AND D-C WORKING VOLTAGE

The measuring circuit used for the SPRF tests was similar to that used in previous SPRF tests.[2] A more convenient analog circuit that measures induced current directly without intermediary computations could not be used because of the late arrival of components from vendors. This analog circuit requires that values of resistance and capacitance be chosen so that their product will approach the circuit time constant, τ.

Table 1

MYLAR CAPACITORS

Capacitor Type	Rated Capacitance (uf)	Maximum Capacitance (uf)	Minimum Capacitance (uf)	WVDC	Applied Voltage
GE-63F22CA103	0.010	0.0105	0.0099	200	0, 40.43, 94.29, 164.90, 205.20
GE-63F23DA103	0.010	0.0110	0.0095	300	0, 70.62, 117.90, 274.10, 280.80
GE-63F15AA123	0.012	0.0129	0.0118	50	0, 10.79, 21.29, 34.19, 47.05
GE-6317BA123	0.012	0.0118	0.0115	100	0, 9.37, 29.80, 70.63, 94.52
GE-63F29BA104	0.100	0.1057	0.0988	100	0, 9.25, 30.84, 99.87
GE-63F40CC104	0.100	0.1011	0.1000	200	0, 47.19, 94.18, 187.90
GE-63F49DA104	0.100	0.1027	0.0964	300	0, 67.10, 114.00, 280.70, 288.50, 289.20
GE-63F26AA124	0.120	0.1194	0.1145	50	0, 10.27, 23.90, 40.40, 47.00
GE-63F60BC684	0.680	0.6606	0.6499	100	0, 9.35, 9.39, 70.42, 94.14
GE-63F51AC105	1.000	0.9970	0.9710	50	0, 10.80, 17.04, 46.69, 47.07, 47.21, 47.[illegible], 47.30
GE-63F88CA105	1.000	1.0360	0.9722	200	0, 40.41, 70.64, 164.90, 186.60, 188.10, 188.30, 188.40, 188.70 188.90, 191.00, 191.10, 193.10, 194.30, 325.90

Table 2

POLYSTYRENE CAPACITORS

Capacitor Type	Rated Capacitance (uf)	Maximum Capacitance (uf)	Minimum Capacitance (uf)	WVDC	Applied Voltage
ARCO 1PT-102	0.001	0.00102	0.00098	100	0, 10.79, 32.19, 70.59, 117.9
ARCO 2PT-102	0.001	0.00104	0.00099	200	0, 47.10, 93.59, 117.6, 194.4
ARCO 4PT-102	0.001	0.00120	0.00098	400	0, 94.23, 183.3, 318.9, 391.2
ARCO 6PT-102	0.001	0.00102	0.00098	600	0, 117.9, 235.9, 593.8
ARCO 1PT-103	0.010	0.01048	0.00991	100	0, 10.87, 29.43, 67.22, 94.56
ARCO 2PT-103	0.010	0.01035	0.00967	200	0, 40.36, 93.38, 117.7, 188.9
ARCO 5PT-103	0.010	0.01023	0.00978	400	0, 94.17, 165, 321.7, 399.9
ARCO 6PT-103	0.010	0.01027	0.00972	600	0, 117.9, 235.9, 593.8
ARCO 1PT-104	0.100	0.10360	0.09824	100	0, 10.82, 29.52, 94.39
ARCO 2PT-104	0.100	0.09985	0.09965	200	0, 40.39, 94.52, 198.9
ARCO 4PT-104	0.100	0.10170	0.09710	400	0, 94.1, 164.9, 362.2, 368.7
ARCO 6PT-104	0.100	0.10070	0.09641	600	0, 117.9, 235.9, 580.9, 582.7, 586.5, 592.4, 593.2, 598.9, 614.9
ARCO 4PT-334	0.330	0.33540	0.33290	400	0, 70.60, 165.3, 325.9, 372.9, 373.2, 375.9, 382.4, 383.5, 384.5, 387.5
ARCO 1PT-504	0.500	0.52430	0.48360	100	0, 9.30, 30.01, 94.04
ARCO 2PT-504	0.500	0.50740	0.48550	200	0, 40.44, 69.91, 118.2, 188.5, 189.1, 191.2

Table 3

CAPACITOR TESTS

Experiment		1		2		3	
Capacitance (uf)	WVDC	Number Tested	Oscillographs Available	Number Tested	Oscillographs Available	Number Tested	Oscillographs Available
MYLAR CAPACITORS							
0.01	200	5	5	0	0	0	0
0.01	300	5	5	0	0	0	0
0.012	50	5	2	0	0	0	0
0.012	100	5	5	0	0	0	0
0.1	100	4	5	0	0	0	0
0.1	200	3	4	0	0	0	0
0.1	300	3	2	0	0	6	5
0.12	50	5	4	0	0	0	0
0.68	100	5	4	0	0	0	0
1.0	50	4	4	8	5	0	0
1.0	200	9	4	8	5	0	0
POLYSTYRENE CAPACITORS							
0.001	100	5	2	0	0	0	0
0.001	200	5	5	0	0	0	0
0.001	400	5	5	0	0	0	0
0.001	600	5	5	0	0	0	0
0.01	100	5	4	0	0	0	0
0.01	200	5	5	0	0	0	0
0.01	400	5	5	0	0	0	0
0.01	600	5	5	0	0	0	0
0.1	100	4	4	0	0	0	0
0.1	200	5	5	0	0	0	0
0.1	400	5	5	0	0	0	0
0.1	600	6	6	8	7	6	4
0.33	400	9	7	8	7	0	0
0.5	100	4	5	0	0	0	0
0.5	200	8	7	4	4	0	0
Ta_2O_5 CAPACITOR							
1.0	50	0	0	0	0	5	4
GLASS CAPACITOR							
0.0015	300	0	0	0	0	4	3
CERAMIC CAPACITOR							
2.2	25	0	0	0	0	3	2
MICA CAPACITOR							
0.075	300	0	0	0	0	6	5

Table 4

NEUTRON-GAMMA RAY TEST CAPACITORS

Capacitor Type	Rated Capacitance (uf)	Maximum Capacitance (uf)	Minimum Capacitance (uf)	WVDC	Applied Voltage
Sprague 150D105X0050AD	1.000	0.9765	0.9713	50	46.09, 46.86,
(Ta_2O_5)	1.000	0.9765	0.9713	50	46.09, 46.86
Corning CY20C (Glass)	0.0015	0.00151	0.00149	300	275.0, 276.6, 280.3
Sprague 5C15 (Ceramic)	2.200	2.026	1.988	25	23.45, 23.92
ARCO SPR-P (Mica)	0.075	0.07398	0.07298	300	280.8, 282.2, 286.6, 288.4

An available IBM 7090 computer program will be used to aid in analyzing the test data.[3] This program delivers a plot which compares the shape of the reactor burst to the capacitor response as a function of time. Any dependence of the induced current on dose-rate, voltage, or geometry is then readily observed in the normalized output.

For several capacitors, the induced current was monitored for a few milliseconds after each burst to measure any long decay time-constant components of the induced current. The relationship between the radiation induced current, i_r, and the current, i, through the termination resistor R_t is:

$$i_r = i + \tau \frac{di}{dt}$$

where $\tau = (Rt + Rc)(C + Cc)$ and Rc and Cc are the resistance and capacitance of the coaxial cables between the component at the reactor and the oscilloscope output.

2. BEHAVIOR UNDER REPEATED IRRADIATION

The efficiency of radiation induced current generation under repeated irradiation was investigated by subjecting five polystyrene and four mylar capacitors to four successive SPRF bursts. The dose rates in these bursts

ranged from approximately 5.94×10^7 to 7.80×10^7 R/second. Capacitance values of the polystyrene capacitors ranged from 0.1 to 0.33 uf with rated voltages up to 600 volts. The mylar capacitors were all 1 uf and rated from 50 to 200 WVDC. For three successive irradiations, the voltages across the capacitors were maintained constant and consistent with the rated voltage. For the fourth irradiation, the voltage across each capacitor was reduced to zero.

Preliminary data analysis does not show a sequential diminishing of the induced current in any of the polystyrene capacitors; however, the mylar capacitors show a slight decrease after successive irradiations. These results do not contradict the space charge buildup found by Coppage and Peterson in polystyrene capacitors. The 600-Kvp pulsed X-ray source[4] used by Coppage and Peterson showed a saturation in conductivity after about ten gamma-ray pulses or a total dose of approximately 20 rads. At the SPRF, the total dose for one burst is at least a factor of 100 larger so that the space charge effects found in the Coppage-Peterson experiment would already by driven into saturation and could not be observed.

3. ALTERATION OF THE NEUTRON-GAMMA RAY RATIO

Capacitors of mylar, polystyrene, mica, glass, solid tantalum, and ceramic were subjected to a series of six bursts with shields located between the capacitors and the reactor. During these bursts, various combinations of lead and polyethelene shields were used to change the neutron-gamma ray ratio over a factor of approximately four. These changes in neutron-gamma ray ratio were accomplished as shown in Figure 1. The computer program mentioned previously will be used to analyze the results for dose-rate, voltage, or geometry dependence of the induced current.

B. LINAC TEST

Mylar, polystyrene, mica, tantalum oxide, glass, and ceramic capacitors were tested with variations of voltage, capacitance, d-c working voltage, and electron dose-rate at the General Atomics' linac. The induced current was monitored through both leads of the capacitor under irradiation. The test circuit contains two CT-2 current probes: one mounted on the voltage side of the exposed capacitor and one on the ground side. These current probes have a nominal insertion impedance of 0.04 ohms and a shunted inductance of 5 microhenries. The test circuit and its equivalent representation are shown in Figure 2.

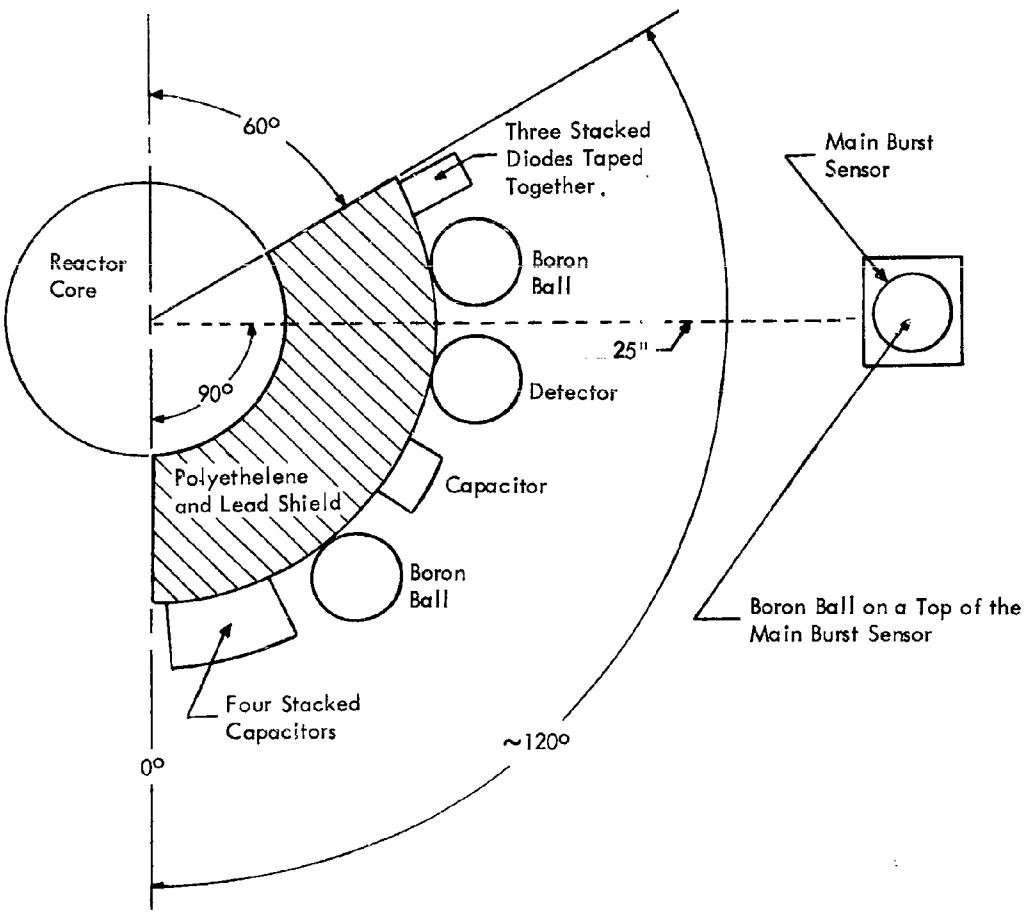

Figure 1. Sample Positions at the SPRF

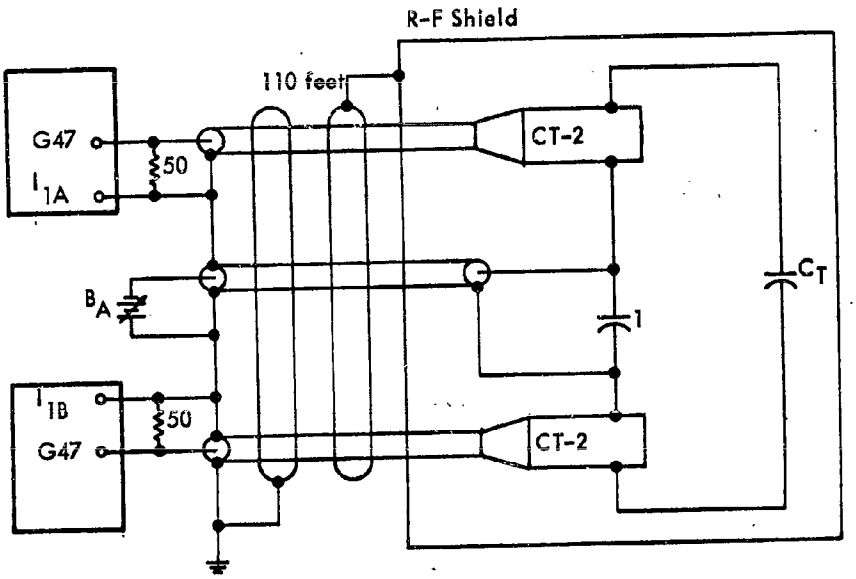

Equivalent Circuit

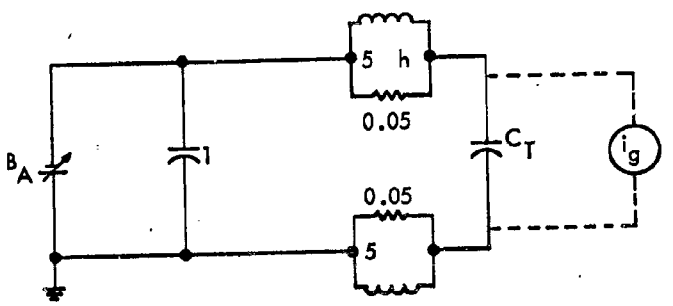

Figure 2. Linac Test Circuit

Positive voltages were applied to the test capacitors over a range of 0 to approximately 1,000 volts dc. The capacitance of the samples ranged from 0.001 to 47 uf. Each capacitor was tested with at least five different voltage settings. Reproducibility tests were performed on selected capacitors with the same applied voltages and approximately the same dose-rate. The dose-rates were varied by irradiating test samples at different positions relative to the exit port of the electron beam tube. The details of the capacitance test are presented in Table 5, which also shows the nominal capacitance values and voltage ratings for each type of dielectric.

Preliminary qualitative observations of the response of each type of capacitor to a square linac pulse are presented in the following paragraphs.

1. CERAMIC CAPACITORS

For small voltages (less than 10 volts) the magnitude of the currents through both capacitor leads was approximately the same. As the voltage was increased, the induced current increased proportionately; however, damped oscillations characteristic of ceramic irradiations appeared. These oscillations had a period of approximately 1 usec. An increase in capacitance from 0.1 to 1 uf increased the period of the damped oscillation to approximately 7.0 usec with a corresponding increase in amplitude. This may be due to the larger circuit time constant for the higher capacitance values.

2. GLASS CAPACITORS

The induced currents through both leads of the glass capacitors differed in magnitude for all positively applied voltages. The current in the high voltage lead was larger. A possible cause may be secondary emission along with ionization of the air surrounding the sample. An increase in capacitance from 300 to 1500 pf produced identical results, indicating no dependence of the induced current on capacitance over this range.

3. TANTALUM CAPACITORS

The tantalum capacitors exhibited an effect not previously observed for a dielectric. The induced current reached a peak value 0.5 to 2.0 usec after the linac pulse, depending upon the nominal size of the capacitor. As the capacitance was increased from 0.22 to 47 uf, the current peak broadened and the exponential decay time correspondingly increased. This effect was most pronounced for pulse widths of about 0.1 to 0.5 usec and was not easily distinguished for the longer pulse widths. A more complete analysis is needed because the large capacitance values used resulted in appreciable circuit time constants. However, the observed effect is definitely a characteristic of the dielectric and is suggestive of a secondary photoconductive current.

Table 5

LINAC CAPACITOR TEST CHART

Dielectric	Irradiation Positions*	Capacitance	WVDC	Voltage Variation	Sample No.
Mica	C	0.13 uf	100	0, 10, 30, 50, 100	1
	C	0.075 uf	300	0, 30, 90, 180, 300	3
	C	0.03 uf	1000	0, 100, 300, 600, 1000	5
	B	0.01 uf	1000	0, 100, 300, 600, 1000	7
Ceramic	A, C	0.1 uf	50	0, 5, 15, 30, 50	9
	A, C	0.47 uf	50	0, 5, 15, 30, 50	11
	A, C	2.2 uf	25	0, 2.5, 7.5, 15, 25	13
	A, C	1 uf	25	0, 2.5, 7.5, 15, 25	15
Glass	A, C	1500 pf	500	0, 50, 150, 300, 500	17
	A, C	300 pf	500	0, 50, 150, 300, 500	21
Tantalum	A	0.22 uf	6	0, 1, 2, 4, 6	23
	A	1 uf	6	0, 1, 2, 4, 6	25
	A	0.22 uf	10	0, 1, 3, 6, 10	27
	A, C	1 uf	10	0, 1, 3, 6, 10	29
	A, C	0.22 uf	15	0, 1.5, 6, 9, 15	31
	A, C	1 uf	15	0, 1.5, 6, 9, 15	33
	A	1 uf	15	0, 1.5, 6, 9, 15	35
	A, C	0.22 uf	20	0, 2, 6, 12, 20	37
	A	1 uf	20	0, 2, 6, 12, 20	39
	A	10 uf	20	0, 2, 6, 12, 20	41
	A, C	1 uf	35	0, 3.5, 10, 20, 35	43
	A, C	10 uf	35	0, 3.5, 10, 20, 35	45
	B	47 uf	35	0, 3.5, 10, 20, 35	47
Polystyrene	C	1 uf	100	0, 10, 30, 60, 100	49
	B	0.001 uf	200	0, 20, 60, 120, 150	52
Mylar	C	0.1 uf	200	0, 20, 60, 100, 200	55
	B	0.01 uf	300	0, 30, 40, 180, 300	58

* Position A dose rate $\cong 2.7 \times 10^9$ R/sec
Position B dose rate $\cong 1.0 \times 10^9$ R/sec
Position C dose rate $\cong 3.3 \times 10^8$ R/sec

4. MICA CAPACITORS

In all mica capacitors irradiated, the induced current was directly proportional to voltage and capacitance. The currents through both capacitor leads reflect the characteristics of the linac pulse identically. At the end of the linac pulse, the current response exhibited a damped oscillation whose amplitude was always small compared to the current observed during the pulse. The period of this oscillation increased with an increase in capacitance and was as long as 1 usec for the highest capacitance value of 0.13 uf.

5. POLYSTYRENE AND MYLAR CAPACITORS

Both polystyrene and mylar capacitors reacted similarly to the linac pulse. Each generated leakage currents that were identical in both capacitor leads, thus ruling out any secondary emission effects or air ionization currents. The induced currents in both types were linear for voltage and capacitance variations. Each type of capacitor was sensitive to the sharp drop in the linac pulse and went into a damped oscillation that had a recovery time of approximately 3 usec. Like the mica capacitors, the period of these damped oscillations increased for an increase in capacitance.

6. SUMMARY

Except for the glass capacitors, the observed currents were well approximated by computations performed prior to the tests for the purpose of setting oscilloscope scale factors. Since these computations were largely based on prior results obtained at the SPRF, good correlation between the linac and the SPRF data is expected.

Typical current response curves for each capacitor type except glass are shown in Figures 3 through 8. The upper two traces are displays of the current through the high potential and ground leads for each capacitor. For comparison, pictures of the linac waveform for each pulse delivered to the sample are shown in the bottom oscillographs. Time references were obtained from a master time mark simultaneously generated on each photograph. The time mark appears as a blank in the trace and is usually referenced in the center of the linac waveform. The deflection sensitivities and applied voltages are shown above each oscillograph of current and linac pulse shape.

The delayed effect of the current response in a tantalum capacitor is readily seen in Figures 4 and 5 by comparing the position of the master time mark in each photograph. The long decay component of the current and the broadening of the current peak with increased capacitance is also evident.

Vertical Scale Factor	10 mv/div
Horizontal Scale Factor	1 usec/div
Applied Voltage	5.00 volts

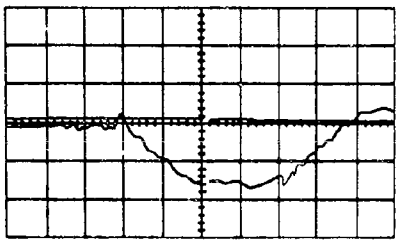

IBM 3-6

Vertical Scale Factor	20 mv/div
Horizontal Scale Factor	1 usec/div
Applied voltage	7.50 volts

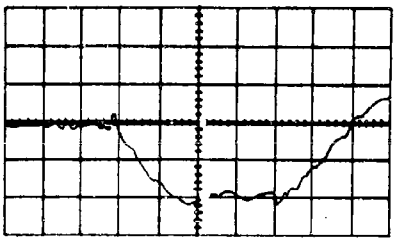

IBM

Figure 3a. High Potential Lead Response

Vertical Scale Factor	10 mv/div
Horizontal Scale Factor	1 usec/div
Applied Voltage	5.00 volts

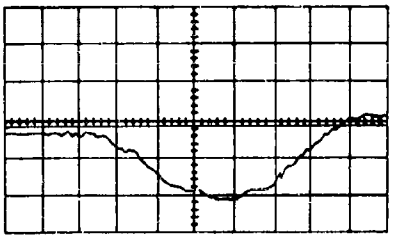

IBM 3-6

Vertical Scale Factor	20 mv/div
Horizontal Scale Factor	1 usec/div
Applied Voltage	7.50 volts

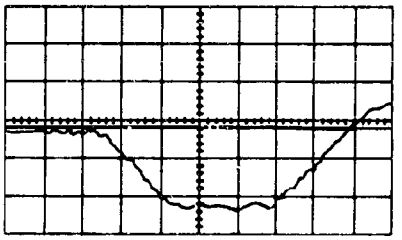

IBM 4-6

Figure 3b. Ground Lead Response

Vertical Scale Factor	0.5 volt/div
Horizontal Scale Factor	1 usec/div

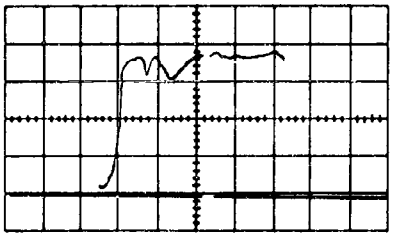

IBM 3-6

Vertical Scale Factor	0.5 volt/div
Horizontal Scale Factor	1 usec/div

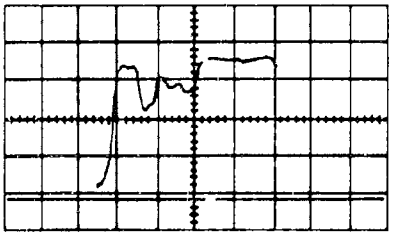

IBM 4-6

Figure 3c. Foil Response

Figure 3. Ceramic Capacitor Response

Vertical Scale Factor	50 mv/div
Horizontal Scale Factor	5 usec/div
Applied Voltage	10 volts

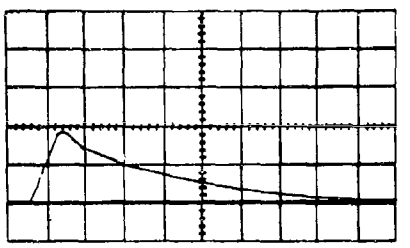

IBM 3-72

Vertical Scale Factor	50 mv/div
Horizontal Scale Factor	5 usec/div
Applied Voltage	20 volts

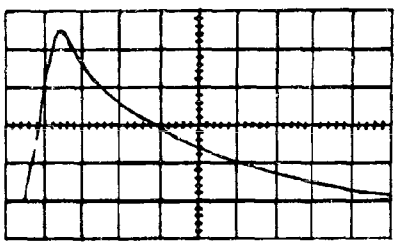

IBM 4-72

Figure 4a. High Potential Lead Response

Vertical Scale Factor	50 mv/div
Horizontal Scale Factor	5 usec/div
Applied Voltage	10 volts

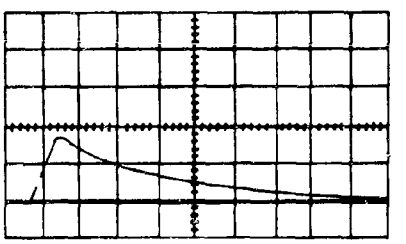

IBM 3-72

Vertical Scale Factor	50 mv/div
Horizontal Scale Factor	5 usec/div
Applied Voltage	20 volts

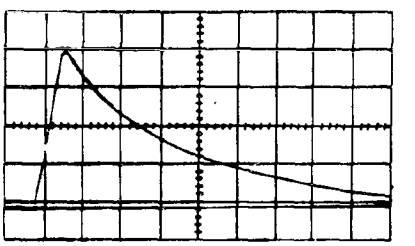

IBM 4-72

Figure 4b. Ground Lead Response

Vertical Scale Factor	0.5 volt/div
Horizontal Scale Factor	1 usec/div

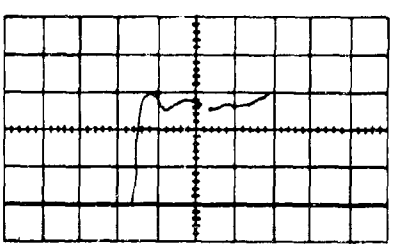

IBM 3-72

Vertical Scale Factor	0.5 volt/div
Horizontal Scale Factor	1 usec/div

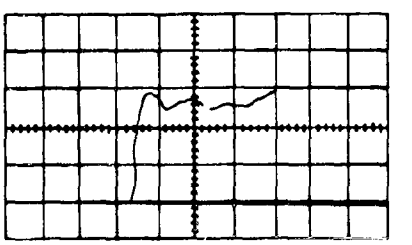

IBM 4-72

Figure 4c. Foil Response

Figure 4. Tantalum Capacitor Response

Vertical Scale Factor	20 mv/div
Horizontal Scale Factor	0.5 usec/div
Applied Voltage	30 volts

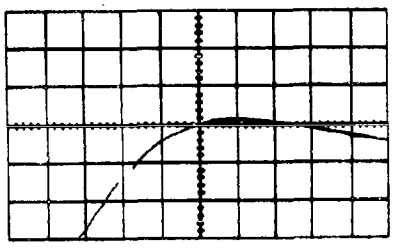

IBM 3-89

Vertical Scale Factor	20 mv/div
Horizontal Scale Factor	50 usec/div

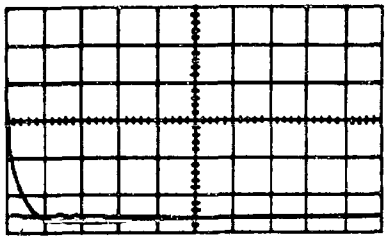

IBM 4-89

Figure 5a. High Potential Lead Response

Vertical Scale Factor	20 mv/div
Horizontal Scale Factor	0.5 usec/div
Applied Voltage	30 volts

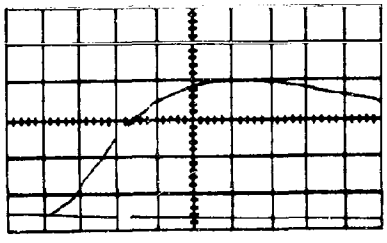

IBM 3-89

Vertical Scale Factor	20 mv/div
Horizontal Scale Factor	50 usec/div

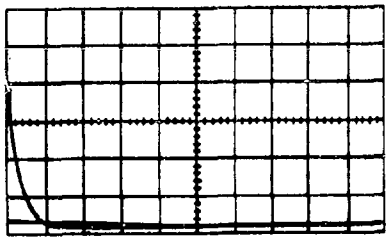

IBM 4-89

Figure 5b. Ground Lead Response

Vertical Scale Factor	0.5 mv/div
Horizontal Scale Factor	1 usec/div

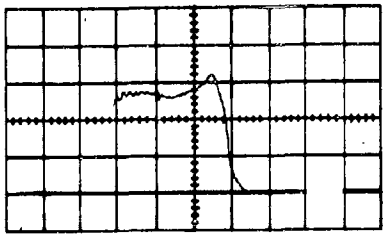

IBM 3-89

Vertical Scale Factor	0.5 mv/div
Horizontal Scale Factor	1 usec/div

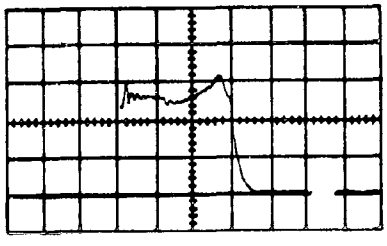

IBM 4-89

Figure 5c. Foil Response

Figure 5. Tantalum Capacitor Response

Vertical Scale Factor	10 mv/div
Horizontal Scale Factor	1 usec/div
Applied Voltage	303 volts

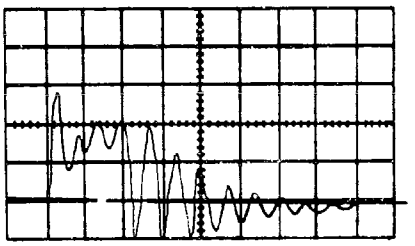

IBM 3-59

Vertical Scale Factor	20 mv/div
Horizontal Scale Factor	1 usec/div
Applied Voltage	598.4 volts

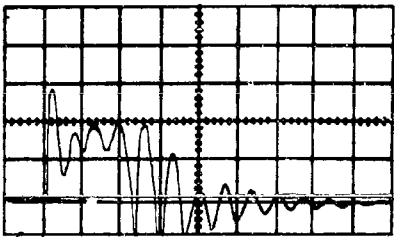

IBM 4-59

Figure 6a. High Potential Lead Response

Vertical Scale Factor	10 mv/div
Horizontal Scale Factor	1 usec/div
Applied Voltage	303 volts

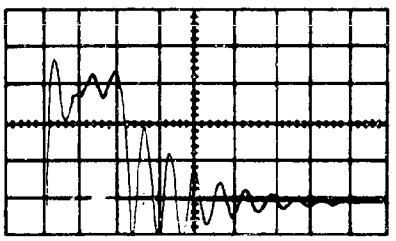

IBM 3-59

Vertical Scale Factor	20 mv/div
Horizontal Scale Factor	1 usec/div
Applied Voltage	598.4 volts

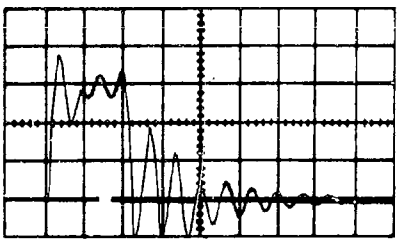

IBM 4-59

Figure 6b. Ground Lead Response

Vertical Scale Factor	0.5 volt/div
Horizontal Scale Factor	0.5 usec/div

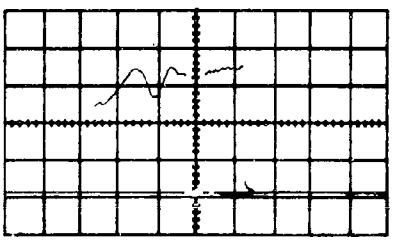

IBM 3-59

Vertical Scale Factor	0.5 volt/div
Horizontal Scale Factor	0.5 usec/div

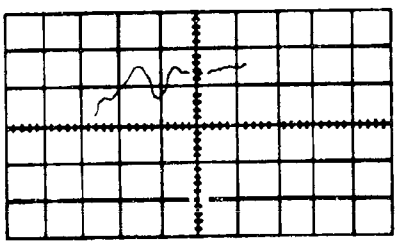

IBM 4-59

Figure 6c. Foil Response

Figure 6. Mica Capacitor Response

Vertical Scale Factor	5 mv/div
Horizontal Scale Factor	0.5 usec/div
Applied Voltage	58.09 volts

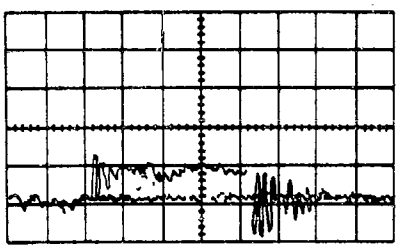

IBM 3-53

Vertical Scale Factor	5 mv/div
Horizontal Scale Factor	0.5 usec/div
Applied Voltage	120 volts

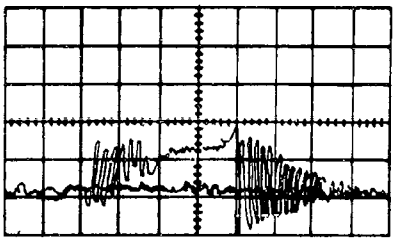

IBM 4-53

Figure 7a. High Potential Lead Response

Vertical Scale Factor	5 mv/div
Horizontal Scale Factor	0.5 usec/div
Applied Voltage	58.09 volts

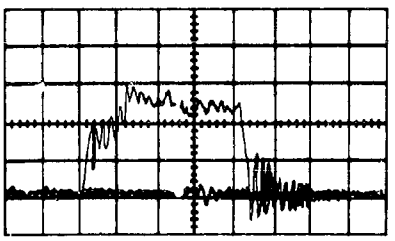

IBM 3-53

Vertical Scale Factor	10 mv/div
Horizontal Scale Factor	0.5 usec/div
Applied Voltage	120 volts

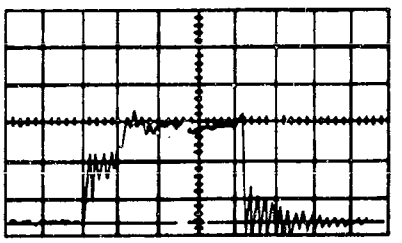

IBM 4-53

Figure 7b. Ground Lead Response

Vertical Scale Factor	0.5 mv/div
Horizontal Scale Factor	0.5 usec/div

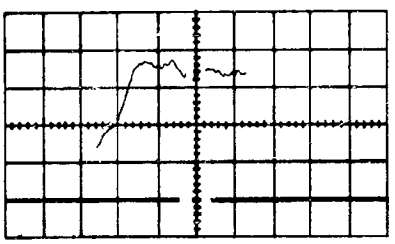

IBM 3-53

Vertical Scale Factor	0.5 volt/div
Horizontal Scale Factor	0.5 usec/div

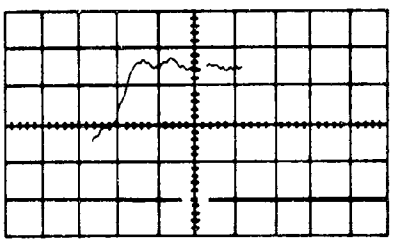

IBM 4-53

Figure 7c. Foil Response

Figure 7. Polystyrene Capacitor Response

Vertical Scale Factor	10 mv/div	Vertical Scale Factor	20 mv/div
Horizontal Scale Factor	0.5 usec/div	Horizontal Scale Factor	0.5 usec/div
Applied Voltage	94.52 volts	Applied Voltage	188.9 volts

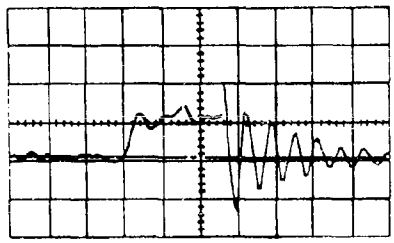

IBM 3-54

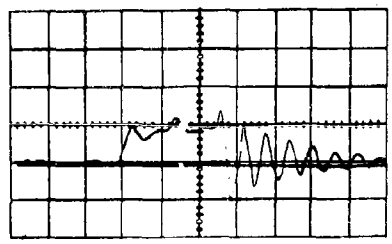

IBM 4-54

Figure 8a. High Potential Lead Response

Vertical Scale Factor	10 mv/div	Vertical Scale Factor	20 mv/div
Horizontal Scale Factor	0.5 usec/div	Horizontal Scale Factor	0.5 usec/div
Applied Voltage	94.52 volts	Applied Voltage	188.9 volts

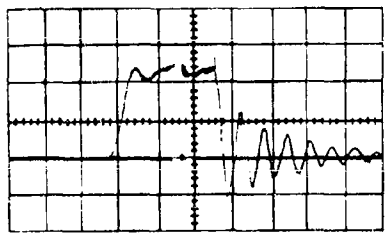

IBM 3-54

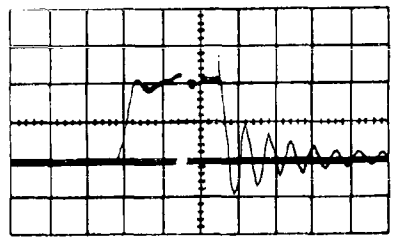

IBM 4-54

Figure 8b. Ground Lead Response

Vertical Scale Factor	0.5 volt/div	Vertical Scale Factor	0.5 volt/div
Horizontal Scale Factor	0.5 usec/div	Horizontal Scale Factor	0.5 usec/div

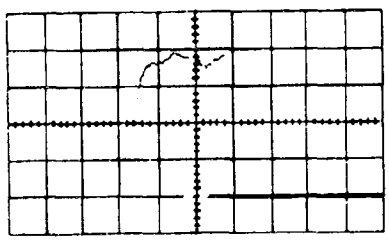

IBM 3-54

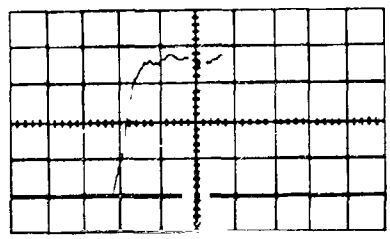

IBM 4-54

Figure 8c. Foil Response

Figure 8. Mylar Capacitor Response

Analysis of the glass capacitor test results showed that the current in the voltage lead differs from the current in the ground lead. The possible causes of this effect are either secondary emission or air ionization.

C. THIN FILM RESISTOR STUDIES

Several thin film resistors were irradiated at a linac to evaluate the radiation hardness of thin film resistors and their substrate. To establish valid testing procedures and to determine the sensitivity of device response to potting, testing was performed with and without potting.

The devices tested, 1k cermet resistors, were fabricated by the Thin Film Electronics Development Department of the IBM Components Division located at Owego, New York. The resistors were made by successively depositing on a glass substrate a layer of SiO, a layer of a 50/50 chrome-SiO mixture, and another layer of SiO. Copper lands were then deposited and tinned, and leads were attached as shown in Figure 9. Using the four connections shown in this figure, measurements were made of the leakage current between two isolated points on the substrate (leads 1 and 2) as well as across the resistor (leads 3 and 4).

The radiation induced leakage current was measured at several device potentials for both the substrate connections and the resistor. In all cases, the current was measured in both leads during a single pulse to determine the significance of replacement current effects. These measurements were also made on a sample potted with paraffin. For all tests, the peak dose rate was about 1.6×10^9 rads/second. These results are shown in Table 6. The polarity of the currents is such that a positive sign means current is flowing away from the component being irradiated. This convention is different from that used elsewhere in this report because it is believed that this approach better illustrates replacement current effects whereas the other approach is better for conductivity modulation in capacitors. All currents were measured at a time mark placed simultaneously on all photographs taken during a single burst.

The large replacement currents observed indicate secondary emission and air ionization effects are the predominant mechanisms underlying the radiation induced behavior of thin film resistors and their substrates. The voltage dependence of the replacement current, as shown in Figure 10 for the substrate, is what would be expected from these types of mechanisms. At zero volt the polarity of the replacement current is such that negative charges are being ejected from the device. As the device becomes positive with respect to ground, the emission of secondary electrons is retarded and the collection of negative ions is enhanced, thereby reducing the replacement current. The reverse is true for a negative bias. Also, as expected from effects of this type, the potential side of the device being tested is more sensitive to changes in device potential than the grounded side.

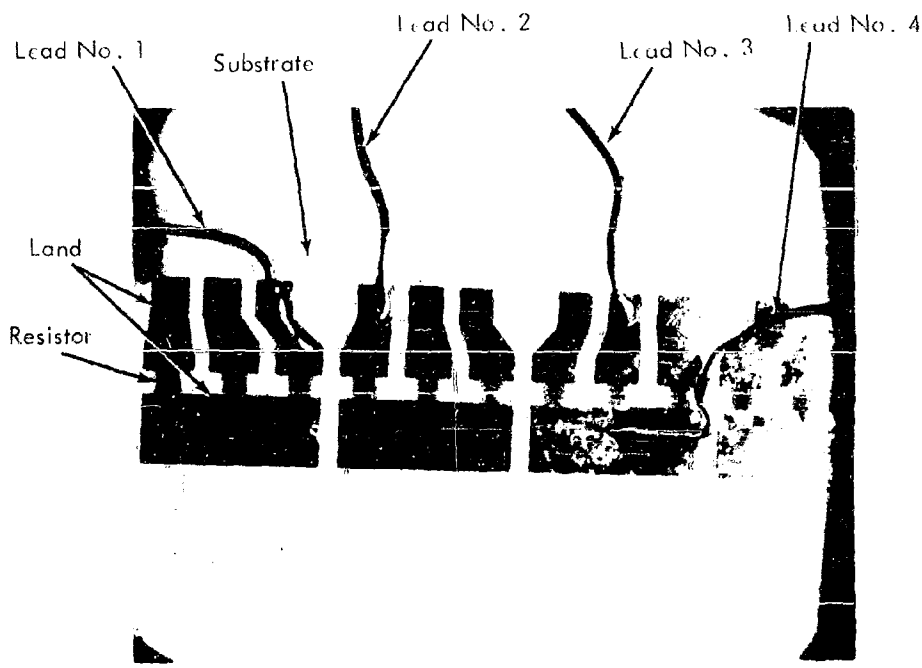

Figure 9. Thin Film Cermet Resistor

Table 6

THIN FILM RESISTOR AND SUBSTRATE TEST RESULTS

Device	Device Potential (volts)	Potential Side Lead (ma)	Ground Side Lead (ma)	Replacement Current (ma)
Unpotted resistor	0	0.56	0.25	0.81
	+2.3	0.48	0.40	0.88
Unpotted substrate	0	0.54	0.60	1.14
	+4.6	0.30	0.59	0.89
	+9.3	0.04	0.61	0.65
	+23.3	-0.84	0.81	-0.03
	-23.5	1.23	0.42	1.65
Potted resistor	0	0.18	0.12	0.30
	+2.3	0.18	0.14	0.32
Potted substrate	0	0.16	0.22	0.38
	+4.6	0.17	0.21	0.38
	+9.3	0.20	0.22	0.42
	+23.4	0.19	0.22	0.41
	-23.5	0.26	0.22	0.48

By repeating the test using thin film resistors potted in paraffin, it was found that the responses observed were quite dependent upon the dielectric media surrounding the device. The smaller signals produced for the potted samples, as listed in Table 6, are to be expected because the paraffin impedes the collection of ions and the emission of secondary electrons. Also, over the voltage range used in the test the currents were much less voltage dependent for the potted resistors than for the unpotted resistors.

The test results indicate that the radiation induced behavior of thin film resistors is dependent upon secondary electron emission and ionization of the media surrounding the resistor. Moreover, effects occurring in the substrate and the resistor lands can be as significant as effects resulting from the resistor itself. Similar types of effects observed in diodes and transistors are discussed in Reference 1.

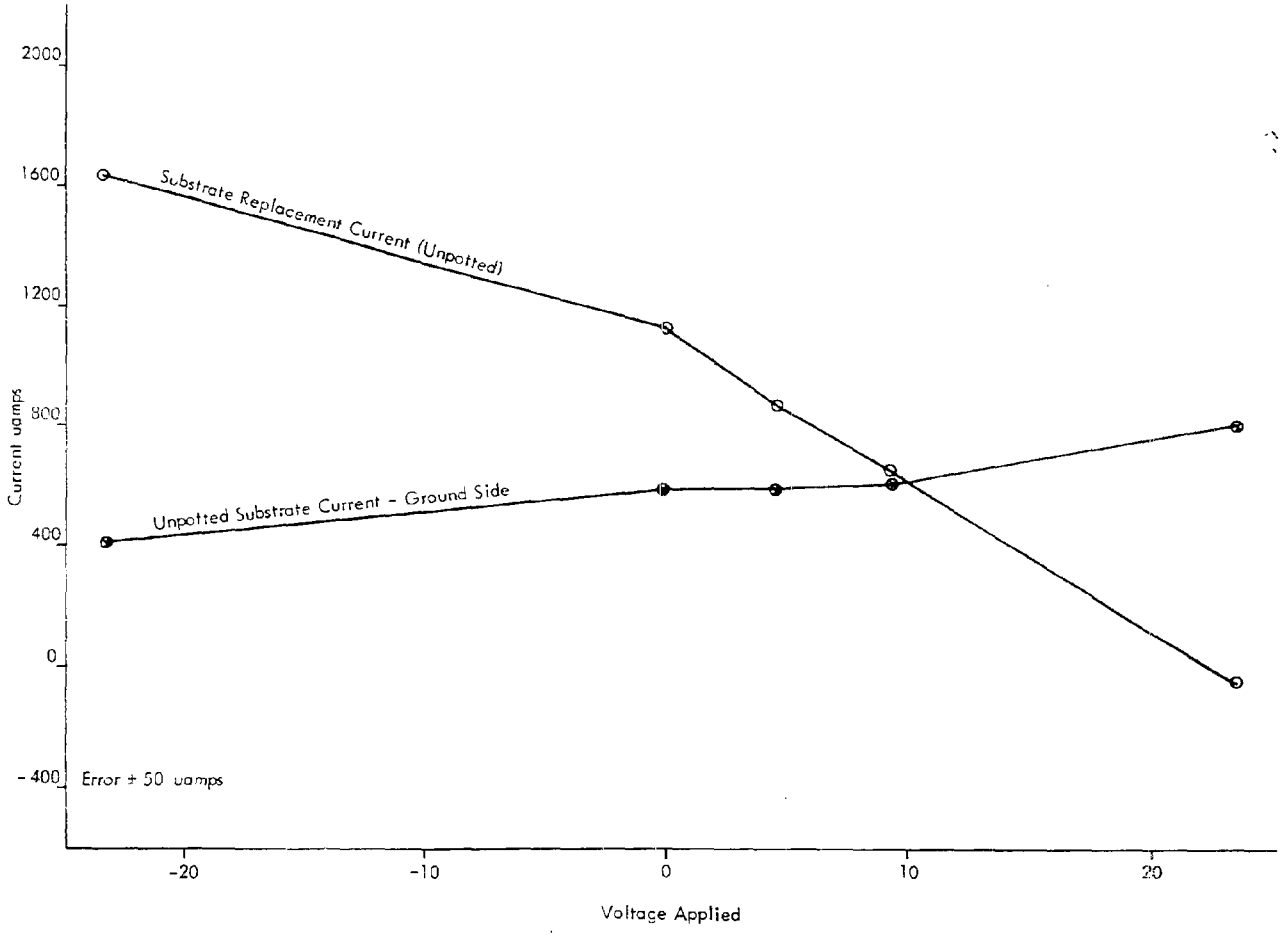

Figure 10. Thin Film Substrate Current versus Device Potential

D. MAGNETIC TAPE AND CORE IRRADIATION

A magnetic tape and two memory core planes were irradiated in December 1964 at the linac to determine whether data stored in these media would be altered or destroyed when exposed to high dose rates.

The magnetic tape test sample was an IBM magnetic tape loaded with one file of binary coded decimal data (high density, 556 bits per inch). This data was recorded on approximately 400 feet of tape giving a test sample of 160 layers (0.3 inch) on the reel of tape. Four different portions of the tape were exposed to a 0.1-usec electron pulse. Test and dosimetry data reduction has not been completed, but the approximate gamma dose rate and beam diameter were 5×10^9 rads/second and 1 inch, respectively.

The test tape was compared with a duplicate tape both before and after irradiation. No errors were detected in the test sample.

The two memory core planes were irradiated in three different areas to expose approximately one-half of the cores of each plane to the electron beam. The first core plane contained 8192 ferrite memory cores. The dimensions of these cores are as follows:

- Inside Diameter — 0.019 inch
- Outside Diameter — 0.032 inch
- Height — 0.0065 inch.

The second memory plane was made up of 4096 two-aperture cores. Data stored in these planes before irradiation will be compared with the data read out after irradiation. Cores in portions of the memory planes not irradiated will be used as control samples.

Test results will be available upon the completion of the data reduction in February and will be presented in a later report.

Section III

SCORRE DOSIMETRY

Section III

SCORRE DOSIMETRY

A. INTRODUCTION

Dosimetry of the two sources of radiation used for radiation effects testing under this contract, i.e., the SPRF and the General Atomics' linac is discussed in this section. For the most part, the techniques used are described in previous IBM reports.[1, 5, 6, 7] However, a recent change in the method of obtaining dosimetry at the linac will be described, including a discussion of erroneous dosimetry data obtained during the linac tests reported in SCORRE Report No. 4, for the 1 November 1963 to 31 January 1964 period.

Except for the SPRF dosimetry, the gamma-ray dosimetry units used in this report are those recommended by the International Commission on Radiological Units and Measurements (ICRU). In the case where incident dose is measured or referenced to, the dose unit used is the roentgen (r) which refers to the ion pairs generated per cubic centimeter in air. When the actual absorbed dose in a material is specified (measured or calculated), the rad unit, equal to 100 ergs/gram actually absorbed in the test sample, is used. The linac dosimetry provides a direct measure of the absorbed dose in test samples, and the appropriate rad unit is specified.

The SPRF gamma dosimetry is reported in ergs/gram (carbon). This unit was originally proposed by the Battelle Memorial Institute and was adopted by IBM 3 years ago. The recent ICRU recommendations are now being adopted to correspond to industry-wide use and the Transient Radiation Effects on Electronics (TREE) Panel recommendations.[9] The unit conversion is expected to be complete by the final report date of this contract. The present pulsed reactor dosimetry unit, the erg/gram (carbon), was derived from the relation: 1 roentgen of gamma ray radiation dose is equivalent to 87.7 ergs/gram deposited in carbon.

A precise correlation between the rad and the roentgen is difficult to ascertain in any real situation. However, for most environments and materials used for pulsed radiation effects testing (e.g., flash X-ray pulsed nuclear reactors and high energy linacs), the conversion 1 roentgen equals (=) 0.9 rad may be used to convert such units with less than 20-percent error.

B. SPRF DOSIMETRY

Routine dosimetry procedures used by IBM at the SPRF are described in various IBM reports.[1, 5, 6, 7] In general, each component subjected to a pulse of radiation is dosimetered by a sulfur pellet for neutron fluence measurement and three glass fluorods for total gamma dose measurements. Burst shapes are determined from the current produced by a phosphor photodiode exposed to each burst.

In six bursts during the SPRF tests, the neutron to gamma ray ratio was varied by using various combinations of lead and polyethelene shields. A variation of neutron flux to gamma ray dose rate ($\dot{N}/\dot{D}$) over a factor of approximately four was achieved in this test. In a previous test, the same variations in polyethelene and lead shields produced a variation in $\dot{N}/\dot{D}$ over a factor of ten. No reason for the difference is apparent except for the relative reactor temperature rises in the two tests. The wider range of $\dot{N}/\dot{D}$ was found when the spread in temperature rises was greatest, apparently indicating a change in relative neutron and gamma ray abundance with reactor temperature rise. However, this argument is not supported by data taken over the wide temperature ranges experienced during several years testing at the SPRF.

Because of difficulties in obtaining consistent results under similar circumstances in different test series. IBM requested that White Sands Missile Range personnel[10] make available to Department of Defense contractors a set of standard shields for which the pulsed reactor leakage flux characteristics are known before a test series is conducted.

A plot of the dosimetry data obtained from Sandia dosimeters used behind various shields during the tests is shown in Figure 11. IBM and Sandia glass fluorod and sulfur dosimetry comparisons made during the tests produced essentially the same results. Uranium, gold, neptunium, and plutonium threshold foil dosimeters were supplied by the Sandia Corporation. The plots of neutron fluence per roentgen for each burst as a function of dosimeter threshold energy are also illustrated in Figure 11.

C. LINAC DOSIMETRY

Dosimetry of the General Atomics' linac beam was performed using lithium-fluoride and glass-fluorod dosimeters. The burst shape was provided by an evacuated set of thin aluminum foils that were placed directly in the linac beam at the end of the beam exit port. The foils were between the beam and the test samples. The secondary emission from the foils produced a current proportional to the beam current. This emission was monitored by an oscilloscope. The foils were calibrated against a large aluminum block which measured the total beam current.

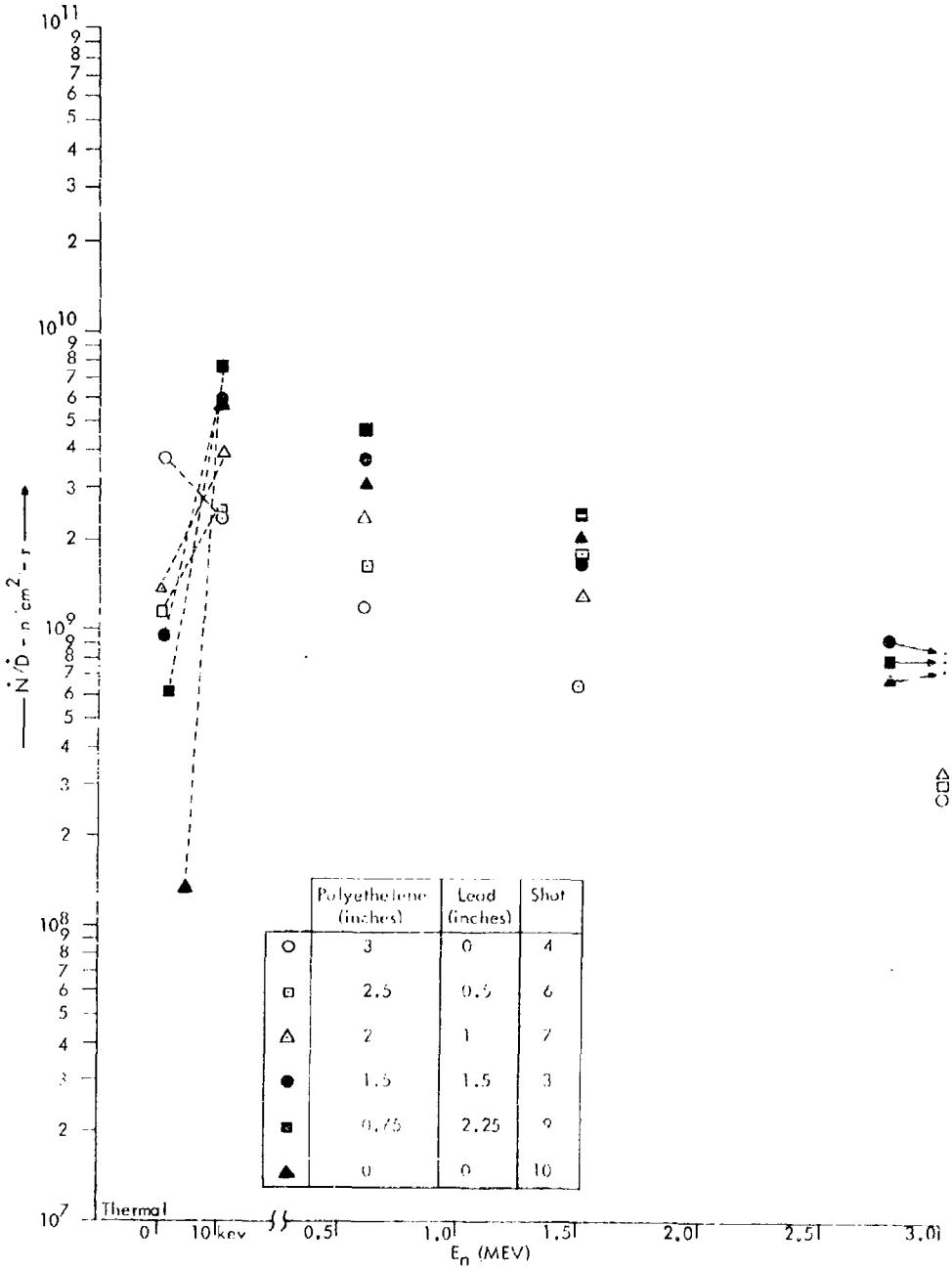

Figure 11. $\dot{N}/\dot{D}$ versus Neutron Dosimeter Threshold Energy

The combination of burst shape obtained from the foils and dosimetric beam maps at various locations along the beam provided a plot of dose rate per unit of beam current (or foil current or voltage) at any position along the beam. The foil current picture taken during an experiment and the plot provided the experimenters with the required dosimetry for each test.

Lithium-fluoride dosimeters were used to obtain the beam maps transverse to the electron beam. The beam cross section is essentially gaussian. The dosimetry maps transverse to the beam direction aid in planning experiments to ensure that sample placement along the beam is compatible with sample size, desired dose rate, and desired uniformity of illumination by the beam across the test sample. Sample locations were restricted by sample size to ensure uniform illumination of all samples across their longest dimension to within ±5 percent.

Peripheral, but very necessary, dosimetry was provided at the test site to make certain that test samples were properly placed in the beam. For beam location, polyvinyl-chloride plastic sheets were exposed (and darkened) to the linac beam at the test sample position immediately before an experiment. This assured the experimenters that the sample was properly placed in the beam.

D. CORRECTIONS TO PREVIOUS LINAC DOSIMETRY

Linac dosimetry data in the SCORRE Fourth Quarterly Progress Report[1] was high by a factor of approximately ten for most of the samples tested at the General Atomics' linac. The actual discrepancy factor varies between approximately five to ten depending upon the position of the sample along the electron beam. More accurate determination of the errors will be presented in forthcoming reports after recent linac test results are analyzed and tentative correlations are established.

The discrepancy arose primarily due to the lack of data regarding the dose rate dependence and the limited range of the glass fluorod dosimetry system available at the time of the test (late 1963). Recently, IBM purchased a lithium-fluoride dosimeter system which has a factor of ten higher total dose range than the glass fluorod system which was available in 1963. Further, recent studies[8] of lithium-fluorid and fluorods show no dose rate dependence of these dosimetry systems up to dose rates of 10^{10} rads/second. The lithium-fluoride system was used in the most recent (1965) linac tests.

Lacking trustworthy dosimeter systems in 1963, the experimenters obtained dose and dose rates by calculating the dose delivered to a thin sample in a high energy electron beam using the following relation:

$$D = \frac{-I}{\rho} \frac{dE}{dx} \int i(t)dt \times 10^{11} \text{ rads},$$

where

D = dose in rads,

$\frac{-IdE}{dx}$ = specific energy loss per electron in $\frac{\text{mev-cm}^2}{\text{gm}}$

i(t) = beam current density in amperes/cm^2,

and

t = time in seconds.

The total current (I) was obtained from the calibrated foils and the current density (i) was evaluated from total current and the area defined by the central darkened region on polyvinyl-chloride sheets exposed at the sample positions. The specific energy loss per electron was determined from published data.

The error may be attributed to misinterpretation of the darkened region on the polyvinyl-chloride sheets. These sheets have a very limited total dose range (approximately 1 to 5×10^6 rads) and readily saturate. The exposed sheets showed several "rings" after exposure (much like a bull's eye), and the central darkened region was assumed to be caused by the majority of the electron flux. The diameter of the beam was, therefore, underestimated, causing the dose per pulse to be overestimated.

For the most recent linac tests performed by IBM under various contracts at two linacs (Natick Army Laboratory and General Atomics), total doses were measured directly, using lithium-fluoride at high current density and long pulse widths and glass fluorods at low current density and short pulse widths. Measurements at both sources indicate that for the geometry used, the electron beam appears to emanate from the linac beam exit port, rather than from a point further out from the exit port as was believed before the lithium-fluoride and fluorods were used. Thus, the discrepancy becomes a function of location of the test samples.

IBM anticipates that recent test results obtained at the General Atomics' linac may be used to correct the previous erroneous data.

Section IV

SUMMARY AND CONCLUSIONS

Section IV

SUMMARY AND CONCLUSIONS

Radiation testing of mylar, polystyrene, mica, tantalum, ceramic, and glass capacitors was completed. The raw data has been organized, and a computer will be used to provide quantitative results. Also, experiments to determine the relative effectiveness of neutron and gamma radiation in producing induced currents have been completed and are being analyzed.

New effects have been observed at the linac. Glass capacitors produced responses with induced currents that are different through both leads to the capacitor. This suggests such mechanisms as secondary emission and air ionization which are not consistent with a conductivity model. The response of tantalum capacitors showed an effect not previously observed for a dielectric. This effect is suggestive of a secondary photoconductive current and is most pronounced for narrow pulse widths such as 0.1 usec.

In the thin film resistor experiments, leakage currents were found to be principally due to secondary emission and air ionization.

No radiation effects were detected in the magnetic tapes. Magnetic core test results will be presented in a later report.

Section V

PROGRAM FOR THE NEXT INTERVAL

Section V

PROGRAM FOR THE NEXT INTERVAL

During the next interval, IBM's major effort will be completing the characterization of all capacitors tested at the SPRF. Analysis of the data resulting from the linac tests will also be completed. Special emphasis will be placed on analyzing the new effects observed in tantalum and glass capacitors. Moreover, a correlation of the induced currents observed at the SPRF and on the linac will be developed.

Data processing of the results of tests on magnetic cores will be completed and presented in the coming period.

Section VI

KEY PERSONNEL

Section VI

KEY PERSONNEL

Listed below are the personnel participating in the Signal Corps Radiation Effects Study and the approx ate number of hours each charged to contract number DA28-043-AMC-00212(E) from 15 June 1964 to 31 December 1964.

Name	Hours Charged
J. M. Boburka	74. 9
P. G. Boczar	88
G. E. Boyd	128
D. R. Carpenter	53
J. F. Cascarino	104. 6
E. R. Covert	119
F. A. Frankovsky	336
J. A. Judd	71
J. L. Knowles	183. 5
W. C. Lamoreaux	24
C. J. Ligas	92. 5
J. A. Martin	145
H. W. Mathers	8
M. Morehouse	83
W. D. Nelson	6
G. A. Price	150
H. N. Rader	241
M. Shatzkes	177
D. C. Sullivan	53
F. C. Tietze	9
C. Shapiro	88
F. A. Nezelek	176
P. Holaska	24
	2434. 5

REFERENCES

1. "Study of Effect of High-Intensity Pulsed Nuclear Radiation on Electronic Parts and Materials (SCORRE)," Report Number Four, 31 March 1964, IBM, Owego, New York.

2. "Study of Effect of High-Intensity Pulsed Nuclear Radiation on Electronic Parts and Materials," Report Number Two, 1 May 1963 to 31 July 1963, IBM, Owego, New York.

3. "Study of Effect High-Intensity Pulsed Nuclear Radiation on Electronic Parts and Materials," Report Number Nine, 1 July 1962 to 30 September 1962, IBM, Owego, New York.

4. Coppage and Peterson, "Temperature Dependence of Photoconductivity Induced in Polystyrene by Transient Radiation," Sandia Reprint, SC-R-64-191, July 1964.

5. "Pulsed Radiation Effects on Aerospace Digital Computers," RTC TDR-63-3051, AFWL, Kirtland AFB, New Mexico, October 1963.

6. "Automated Digital Computer Program for Determining Responses of Electronic Systems to Transient Nuclear Radiation," WL TDR-64-62, Volume 1, AFWL, Kirtland AFB, New Mexico, July 1964.

7. NBS Handbook 84, U. S. Department of Commerce, Washington D. C., see also H. H. Rossi, "New ICRU Recommendations on Radiation Quantities and Units," Nucleonics, Volume 21, Page 75, July 1963.

8. Edgerton, Germeshausen, and Grier, "Energy and Rate Dependence Studies Final Report, "S-237-R, Contract DA-149-186-ORD-1059, undated (approximately January 1964).

9. TREE Handbook, DASA 1420, Battelle Memorial Institute, Columbus, Ohio.

10. Leo Flores, White Sands Missile Range (personal communication).

AD_____ Accession No _____
International Business Machines
FSD Space Guidance Center
Owego, New York

STUDY OF EFFECT OF HIGH-INTENSITY
PULSED NUCLEAR RADIATION ON
ELECTRONIC PARTS AND MATERIALS
(SCORE)

First Semiannual Progress Report (Unclassified)
19 January 1965
Contract No. DA28-043-AMC-00212(E)

Radiation testing of ceramic, glass, tantalum, mica, polystyrene, and mylar capacitors is complete. Data analysis is not complete. New effects were observed when testing glass and tantalum capacitors. Leakage currents in irradiated thin film resistors are principally due to secondary emission and air ionization. No data errors were detected on a magnetic tape that was irradiated. Dosimetry techniques are described, and errors in previous linac dosimetry are discussed.

UNCLASSIFIED

1. Effect of High-Intensity Pulsed Nuclear Radiation on Electronic Parts and Materials
2. Ceramic, glass, tantalum, mica, polystyrene, and mylar capacitors. Thin film resistors. Magnetic tapes and cores.
3. Contract No. DA28-043-AMC-00212(E)

AD_____ Accession No _____
International Business Machines
FSD Space Guidance Center
Owego, New York

STUDY OF EFFECT OF HIGH-INTENSITY
PULSED NUCLEAR RADIATION ON
ELECTRONIC PARTS AND MATERIALS
(SCORE)

First Semiannual Progress Report (Unclassified)
19 January 1965
Contract No. DA28-043-AMC-00212(E)

Radiation testing of ceramic, glass, tantalum, mica, polystyrene, and mylar capacitors is complete. Data analysis is not complete. New effects were observed when testing glass and tantalum capacitors. Leakage currents in irradiated thin film resistors are principally due to secondary emission and air ionization. No data errors were detected on a magnetic tape that was irradiated. Dosimetry techniques are described, and errors in previous linac dosimetry are discussed.

UNCLASSIFIED

1. Effect of High-Intensity Pulsed Nuclear Radiation on Electronic Parts and Materials
2. Ceramic, glass, tantalum, mica, polystyrene, and mylar capacitors. Thin film resistors. Magnetic tapes and cores.
3. Contract No. DA28-043-AMC-00212(E)

AD ______________ Accession No. ______________

International Business Machines
FSD Space Guidance Center
Owego, New York

STUDY OF EFFECT OF HIGH-INTENSITY
PULSED NUCLEAR RADIATION ON
ELECTRONIC PARTS AND MATERIALS
(SCORRE)

First Semiannual Progress Report (Unclassified)
19 January 1965
Contract No. DA28-043-AMC-00212(E)

Radiation testing of ceramic, glass, tantalum, mica, polystyrene, and mylar capacitors is complete. Data analysis is not complete. New effects were observed when testing glass and tantalum capacitors. Leakage currents in irradiated thin film resistors are principally due to secondary emission and air ionization. No data errors were detected on a magnetic tape that was irradiated. Dosimetry techniques are described, and errors in previous linac dosimetry are discussed.

UNCLASSIFIED

1. Effect of High-Intensity Pulsed Nuclear Radiation on Electronic Parts and Materials
2. Ceramic, glass, tantalum, mica, polystyrene, and mylar capacitors. Thin film resistors. Magnetic tapes and cores.
3. Contract No. DA28-043-AMC-00212(E)

AD ______________ Accession No. ______________

International Business Machines
FSD Space Guidance Center
Owego, New York

STUDY OF EFFECT OF HIGH-INTENSITY
PULSED NUCLEAR RADIATION ON
ELECTRONIC PARTS AND MATERIALS
(SCORRE)

First Semiannual Progress Report (Unclassified)
19 January 1965
Contract No. DA28-043-AMC-00212(E)

Radiation testing of ceramic, glass, tantalum, mica, polystyrene, and mylar capacitors is complete. Data analysis is not complete. New effects were observed when testing glass and tantalum capacitors. Leakage currents in irradiated thin film resistors are principally due to secondary emission and air ionization. No data errors were detected on a magnetic tape that was irradiated. Dosimetry techniques are described, and errors in previous linac dosimetry are discussed.

UNCLASSIFIED

1. Effect of High-Intensity Pulsed Nuclear Radiation on Electronic Parts and Materials
2. Ceramic, glass, tantalum, mica, polystyrene, and mylar capacitors. Thin film resistors. Magnetic tapes and cores.
3. Contract No. DA28-043-AMC-00212(E)

AD ______________ Accession No. ______________

International Business Machines
FSD Space Guidance Center
Owego, New York

STUDY OF EFFECT OF HIGH-INTENSITY
PULSED NUCLEAR RADIATION ON
ELECTRONIC PARTS AND MATERIALS
(SCORRE)

First Semiannual Progress Report (Unclassified)
19 January 1965
Contract No. DA28-043-AMC-00212(E)

Radiation testing of ceramic, glass, tantalum, mica, polystyrene, and mylar capacitors is complete. Data analysis is not complete. New effects were observed when testing glass and tantalum capacitors. Leakage currents in irradiated thin film resistors are principally due to secondary emission and air ionization. No data errors were detected on a magnetic tape that was irradiated. Dosimetry techniques are described, and errors in previous linac dosimetry are discussed.

UNCLASSIFIED

1. Effect of High-Intensity Pulsed Nuclear Radiation on Electronic Parts and Materials
2. Ceramic, glass, tantalum, mica, polystyrene, and mylar capacitors. Thin film resistors. Magnetic tapes and cores.
3. Contract No. DA28-043-AMC-00212(E)

AD ______________ Accession No. ______________

International Business Machines
FSD Space Guidance Center
Owego, New York

STUDY OF EFFECT OF HIGH-INTENSITY
PULSED NUCLEAR RADIATION ON
ELECTRONIC PARTS AND MATERIALS
(SCORRE)

First Semiannual Progress Report (Unclassified)
19 January 1965
Contract No. DA28-043-AMC-00212(E)

Radiation testing of ceramic, glass, tantalum, mica, polystyrene, and mylar capacitors is complete. Data analysis is not complete. New effects were observed when testing glass and tantalum capacitors. Leakage currents in irradiated thin film resistors are principally due to secondary emission and air ionization. No data errors were detected on a magnetic tape that was irradiated. Dosimetry techniques are described, and errors in previous linac dosimetry are discussed.

UNCLASSIFIED

1. Effect of High-Intensity Pulsed Nuclear Radiation on Electronic Parts and Materials
2. Ceramic, glass, tantalum, mica, polystyrene, and mylar capacitors. Thin film resistors. Magnetic tapes and cores.
3. Contract No. DA28-043-AMC-00212(E)

UNITED STATES ARMY ELECTRONICS LABORATORIES,
STANDARD DISTRIBUTION LIST,
RESEARCH AND DEVELOPMENT CONTRACT REPORTS

	Copies
Office of the Assistant Secretary of Defense (R&E) Room 3E1065 ATTN: Technical Library The Pentagon Washington 25, D. C.	1
Chief of Research and Development Department of the Army Washington 25, D. C.	2
Commanding General U. S. Army Materiel Command ATTN: R&D Directorate Washington, D. C. 20315	2
Commander, Defense Documentation Center ATTN: TISIA Cameron Station, Building 5 Alexandria, Virginia 22314	10
Commanding Officer U. S. Army Combat Developments Command ATTN: CDCMR-E Fort Belvoir, Virginia	1
Commanding General U. S. Army Combat Developments Command Communications-Electronics Agency Fort Huachuca, Arizona	1
Chief, U. S. Army Security Agency ATTN: ACofS, Gs (Technical Library) Arlington Hall Station Arlington 12, Virginia	2
Deputy President U. S. Army Security Agency Board Arlington Hall Station Arlington 12, Virginia	1

	Copies
Commanding Officer Harry Diamond Laboratories Connecticut Avenue & Van Ness St., N.W. Washington 25, D.C.	1
Director, U.S. Naval Research Laboratory ATTN: Code 2027 Washington, D.C. 20390	1
Commanding Officer and Director U.S. Navy Electronic Laboratory ATTN: Library San Diego 52, California	1
Systems Engineering Group (SEPIR) Wright-Patterson Air Force Base, Ohio 45433	1
Director, Materiel Readiness Directorate Hq., U.S. Army Electronics Command ATTN: AMSEL-MR Fort Monmouth, New Jersey 07703	1
Air Force Cambridge Research Laboratories ATTN: CRXL-R L.G. Hanscom Field Bedford, Massachusetts	2
Electronic Systems Division (AFSC) Scientific & Technical Information Division (ESTI) L.G. Hanscom Field Bedford, Massachusetts 01731	2
Rome Air Development Center ATTN: RAALD Griffiss Air Force Base, New York	1
Advisory Group on Electron Devices 346 Broadway, 8th Floor New York, New York 10013	3
AFSC Scientific/Technical Liaison Office U.S. Naval Air Development Center Johnsville, Pennsylvania	1

	Copies
USAEL Liaison Office Rome Air Development Center ATTN: RAOL Griffiss Air Force Base, New York 13442	1
NASA Representative (SAK/DL) Scientific and Technical Information Facility P.O. Box 5700 Bethesda, Maryland 20014	2
Commander U.S. Army Research Office (Durham) Box CM - Duke Station Durham, North Carolina	1
Commanding Officer U.S. Army Engineer Research & Development Laboratories ATTN: STINFO Branch Fort Belvoir, Virginia 22060	2
Marine Corps Liaison Office U.S. Army Electronics Laboratories ATTN: AMSEL-RD-LNR Fort Monmouth, New Jersey 07703	1
AFSC Scientific/Technical Liaison Office U.S. Army Electronics Laboratories ATTN: AMSEL-RD-LNA Fort Monmouth, New Jersey 07703	1
Director U.S. Army Electronics Laboratories ATTN: AMSEL-RD-DR/DE Fort Monmouth, New Jersey 07703	1
Director U.S. Army Electronics Laboratories ATTN: Technical Documents Center Fort Monmouth, New Jersey 07703	1
Director U.S. Army Electronics Laboratories ATTN: AMSEL-RD-ADO-RHA Fort Monmouth, New Jersey 07703	1

	Copies
Commanding Officer U. S. Army Electronics Research & Development Activity ATTN: AMSEL-RD-WS-A White Sands, New Mexico 88002	1
Hq., U. S. Army Electronics Command Commodity Management Office ATTN: AMSEL-TE Fort Monmouth, New Jersey 07703	1
EL Memorandum No. 335-6, C3 17 June 1964	
Director U. S. Army Electronics Laboratories ATTN: AMSEL-RD-PE (Division Director) ATTN: AMSEL-RD-P (Department Director) ATTN: AMSEL-RD-PE (Dr. E. Both) Fort Monmouth, New Jersey	 1 1 1
Massachusetts Institute of Technology Lincoln Laboratory ATTN: Document Librarian 244 Wood Street Lexington, Massachusetts	1
Nuclear Engineering Directorate Picatinny Arsenal, Building 65 ATTN: Mr. R. K. Benson (SMUPA-TV) Dover, New Jersey	2
Commanding Officer STEWS-AMTED-E ATTN: NEL-Mr. G. Elder White Sands Missile Range, New Mexico	1
Commanding General U. S. Army Materiel Command ATTN: AMCRD-DN Washington, D. C. 20315	1
Commanding Officer U. S. Naval Applied Science Laboratory U. S. Naval Base Brooklyn 1, New York	1

	Copies
Commanding Officer and Director U. S. Naval Radiological Defense Laboratory ATTN: Mr. H. A. Zagorites San Francisco, California 94135	1
Commanding Officer U. S. Naval Weapons Evaluation Facility ATTN: Code 3434 Kirtland Air Force Base, New Mexico 87117	1
Commanding Officer Naval Aviation Material Center Philadelphia, Pennsylvania	1
Rome Air Development Center ATTN: EMERM Griffiss Air Force Base, New York 13442	1
Rome Air Development Center ATTN: EMEAM Griffiss Air Force Base, New York 13442	1
Brookhaven National Laboratory Tech Info Division, Documents Group ATTN: Dr. G. H. Vineyard Upton, Long Island, New York	1
Director Defense Atomic Support Agency ATTN: RANU Washington, D. C. 20301	1
Director Defense Intelligence Agency ATTN: DIAAP-1K2 Washington, D. C. 22212	1
Director Advanced Research Projects Agency ATTN: Major G. L. Sherwood Washington, D. C. 20301	2
Admiral Corporation ATTN: Mr. R. Whitner 3800 Cortland Street Chicago 47, Illinois	1

	Copies
Bell Telephone Laboratories, Inc. 463 West Street New York, New York	1
Burroughs Corporation Defense and Space Group ATTN: Mr. A. L. Long Central Avenue & Route 202 Paoli, Pennsylvania	1
General Atomic Division General Dynamics Corporation ATTN: Dr. V. A. J. Van Lint, Dr. J. L. Russell 10955 John Jay-Hopkins Drive P. O. Box 608 San Diego, California	2
General Electric Company Military Communication Department ATTN: Mr. L. Dee Court Street Syracuse, New York	1
General Electric Company Re-Entry Systems Department ATTN: Mr. J. F. Duncan 3198 Chestnut Street Philadelphia 1, Pennsylvania	1
General Electric Facility Bldgs.10 and 12, Receiving Tube Department ATTN: Mr. Daniel D. Mickey Old Hartford Road Owensboro, Kentucky	1
Lockheed Aircraft Corporation Lockheed Missiles & Space Company Division ATTN: Mr. Fred Barline, Dept. 5872 1111 Lockheed Way Sunnyvale, California	1
Martin Marietta Corporation Friendship International Airport Baltimore, Maryland	1

	Copies
Martin Marietta Corporation Middle River, Baltimore, Maryland	1
Motorola Semiconductor Projects Division ATTN: Mr. Joseph L. Flood 5005 East McDowell Road Phoenix, Arizona	1
New York University ATTN: Mr. H. Kallmann, Physics Dept. Washington Square New York 3, New York	1
North American Aviation Corporation Autonetics Division 3370 Machoma Avenue Anaheim, California	1
Northrop Corporation Ventura Division ATTN: Dr. T.M. Hallman 1515 Rancho Conejo Boulevard Newbury Park, California	1
Battelle Memorial Institute ATTN: Mr. D.C. Jones 505 King Avenue Columbus, Ohio 43201	2
TRW Space Technology Laboratories, Inc. Thompson-Ramo Wooldridge, Inc. One Space Park Redondo Beach, California	1
Sperry Microwave Electronics Company ATTN: Dr. Gordon R. Harrison P.O. Box 1828 Clearwater, Florida	1
Stevens Institute of Technology ATTN: Dr. E. Hanley 501 and 711 Hudson Street Hoboken, New Jersey	1

	Copies
Varian Associates ATTN: Dr. J. Haimson 611 Hansen Way Palo Alto, California	1
Commanding Officer U. S. Army Materiel Command Harry Diamond Laboratories ATTN: Mr. Peter Haas, Chief, Nuclear Vulnerability Branch (230) Connecticut Avenue and Van Ness Street N. W. Washington 25, D. C.	1
Commanding Officer U. S. Army Electronics Research and Development Activity ATTN: AMSEL-RD-WS-A White Sands, New Mexico 88002	1
Commanding Officer Naval Ordnance Laboratory ATTN: Dr. Bryant Corona, California	1
Commander Naval Ordnance Laboratory, White Oak ATTN: Mr. Grantham Silver Spring, Maryland	1
Commanding Officer Air Force Special Weapons Center ATTN: T. Sgt. Paul Sykes Kirtland Air Force Base, New Mexico 87117	1
Air Force Weapons Laboratory ATTN: (WLL) Kirtland Air Force Base, New Mexico 87117	1
AFSWC (WLRPA) Kirtland Air Force Base, New Mexico 87117	1
AFSWC (WLDN) Kirtland Air Force Base, New Mexico 87117	1

	Copies
General Electric Microwave Department ATTN: Mr. A. Hodges 130 Saratoga Road Schenectady, New York	1
Hughes Aircraft Company Ground Systems Group 1901 W. Malvern Avenue Fullerton, California	1
International Business Machines Corporation Federal Systems Division ATTN: Mr. Bohan Route 17C Owego, New York	1
Radiation Effects Information Center Battelle Memorial Institute ATTN: Mr. E.N. Wyler 505 King Avenue Columbus 1, Ohio	1
Northrop Corporation Ventura Division ATTN: Dr. D.A. Hicks 8000 Woodley Avenue Van Nuys, California	1
Applied Physics Laboratory Johns Hopkins University 8621 Georgia Avenue Silver Spring, Maryland ATTN: Mr. Robert Frieberg Via: BuWeps Representative, APL/JHU Silver Spring, Maryland	1
General Dynamics/Fort Worth Convair Division ATTN: Mr. E.L. Burkhard Grants Land Fort Worth 1, Texas	1

	Copies
President Sandia Corporation ATTN: S. C. Rogers, 5312 Sandia Base Albuquerque, New Mexico	1
Director U. S. Army Electronics Laboratories ATTN: AMSEL-RD-PEE (Mr. C. P. Lascaro) Fort Monmouth, New Jersey	1
Director U. S. Army Electronics Laboratories ATTN: AMSEL-RD-PEE (Mr. W. Schlosser) Fort Monmouth, New Jersey	2
U. S. Army Picatinny Arsenal ATTN: Mr. J. W. Gregorits Chief, Advanced Concepts Section Dover, New Jersey	1
The Boeing Company, Aerospace Division Physics Technology Dept. ATTN: Dr. Glenn Keistor 7755 E. Marginal Way Seattle 8, Washington	1
D. M. Newell, Dept. 52-10, 204 Lockheed Missiles and Space Company 3251 Hanover Street Palo Alto, California	1
Dr. B. Sussholz Space Technology Laboratories, Inc. One Space Park Redondo Beach, California	1
President Sandia Corporation ATTN: A. W. Snyder, 5313 Sandia Base Albuquerque, New Mexico	1